IOP Conf. Series: Materials Science and Engineering **297** (2018) 012065 doi:10.1088/1757-899X/297/1/012065

Experimental study on the heat transfer enhancement of the effect of teardrop protrusion-to-protrusion spacing

O. Yemin, M. Wae-Hayee*, and C. Nuntadusit

Energy Technology Research Center and Department of Mechanical Engineering, Faculty of Engineering, Prince of Songkla University, Hat Yai, Songkhla 90112, Thailand

* Corresponding Author: wmakatar@eng.psu.ac.th

Abstract. An experimental analysis was presented for heat transfer on the surface of teardrop protrusions with an inline arrangement. The air flow was passed through perpendicularly over the single row of 5 protrusions in the rectangular wind tunnel. The protrusion height from the bottom of wind tunnel was H/D=0.2 and the spacing of teardrop protrusion-to-protrusion was adjusted by four different spacing cases such as S/D= 1.125, 1.25, 1.5 and 2. The spacing can affect heat transfer enhancement and flow characteristics. Therefore, the spacing which was analysed in this study considered four cases because of experimental limitations. The temperature distributions of surface with protrusions was detected by using the thermochromic liquid crystal sheet (TLC) at Re_H=20,000. Image processing was used to evaluate distribution of Nusselt number. The result shows that the highest average Nusselt number was found in S/D=1.125D case.

1. Introduction

Using passive heat transfer enhancement techniques such as ribs, pin fins, vortex generators, dimpled surface and surface with arrays of protrusions can enhance heat transfer in internal flow passages and can increase secondary flow and turbulence level for mixing enhancement. These kinds of flow can remove heat away from surfaces. Therefore, this passive heat transfer enhancement techniques were used in many industrial applications such as cooling of turbine airfoil, combustion chamber, electronics cooling devices and heat exchangers. Dimples and protrusions are an attractive method for internal cooling due to significant enhancement of turbulence level, enhancement in heat transfer convection with minimal pressure drop penalties and form multiple vortex pair that enhance Nusselt number distributions.

Acharya et al. [1] investigated experimentally and numerically on heat transfer and flow structure for four types of dimple shape (square, triangular, circular, and teardrop) in square internal passage. They showed that the teardrop dimple was the highest heat/mass transfer among four dimples by comparing with both experimental and numerical results. And then, the triangular dimple was the lowest heat transfer enhancement. For flow pattern, the circular and teardrop geometries have single vortex roll that was formed in wake region, but square dimple showed no noticeable vortex roll.

The flow and heat transfer characteristics of teardrop dimple and protrusion was investigated and compared with hemispherical dimple/protrusion by Xie et al. [1]. They showed the thermal performance for teardrop dimple and protrusion is higher than hemispherical dimple and protrusion for

lower Reynold number and thermal performance increased gradually as the centre moves downwards for the teardrop dimple/protrusion.

Rao et al. [4] investigated an experiment and a numerical study on the heat transfer of turbulent flow in channel with staggered arrangement of spherical and teardrop dimples in 11 rows. They found that heat transfer performance of teardrop dimple was distinctively higher than spherical dimple. Although many researchers have studied about heat transfer and flow characteristics with many dimple and protrusion row on the surface, it is still difficult to describe the phenomenon of flow and heat transfer characteristics. Therefore, the heat transfer characteristics with single protrusion row over the surface was researched in this work.

Many literatures have been analysed about the different arrangement of dimpled and protruded surface. The aim of this work was to investigate experimentally the effect of spacing between protrusion-to-protrusion on heat transfer characteristics with a single row of 5 protrusions. The spacing can affect the different value of heat transfer enhancement. The different four spacings in this work was considered according to experimental dimensions.

1.1. Model of protrusion

Figure 1 shows the model of 5 protrusions which was made by plastic and installed on the internal surface of rectangular wind tunnel. The air with fully developed flow passes through the tear drop protrusions. The origin of Cartesian coordinate system was existed at the centre of middle dimple such as X-axis is the along the flow direction of wind tunnel, Y-axis is the rectangular wind tunnel height direction and Z-axis is normal direction to the flow.

The details of protrusion are shown in figure 2. The spherical with the radius of r =0.725D and the projected diameter on the surface was D=26.4mm. The height of protrusion from the surface was 0.2D. The spacing between protrusion-to-protrusion was varied with S/D= 1.125, 1.25, 1.5 and 2. The Reynolds number of mainstream air inside the wind tunnel based on the hydraulic diameter of wind tunnel was fixed at Re_H=20,000 at the middle of wind tunnel by using Pitot tube to measure velocity. The position of Pitot tube is shown in figure 4.

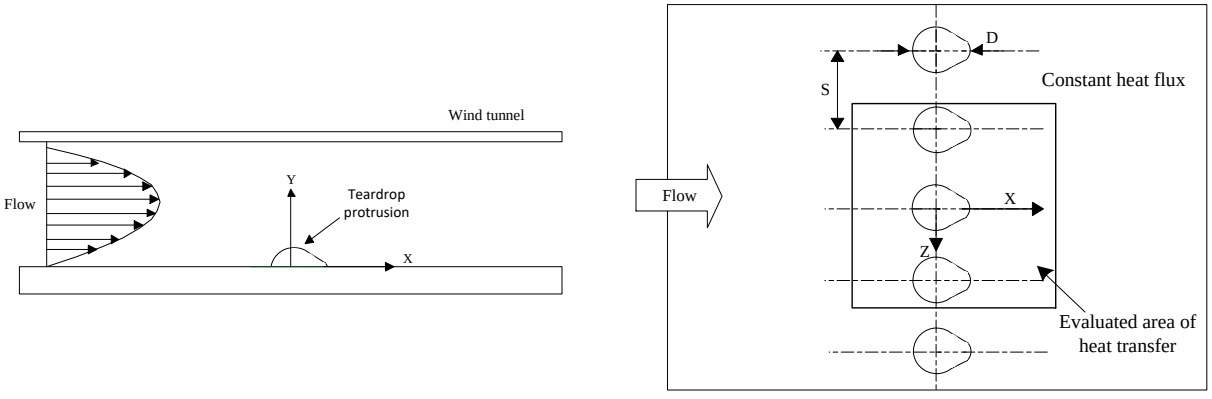

(a) Side view **(b)** Top View

Figure 1. The model of investigation for teardrop test section.

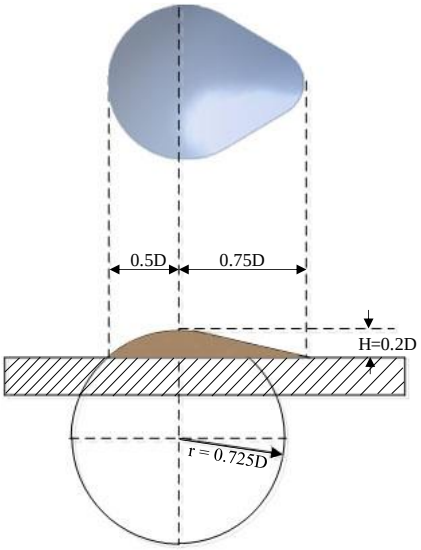

Figure 2. The detail of protrusion.

1.2. Wind tunnel

Figure 3 shows the details of wind tunnel in the experiment. The rectangular wind tunnel was designed with three parts: the upstream of test section (1700 *mm*) that was sufficient distance to get fully developed flow, test section (280*mm*) where was formed teardrop protrusions and downstream of test section where the air was leaved out from the wind tunnel. The wind tunnel height was 26.4 *mm* (1*D*).

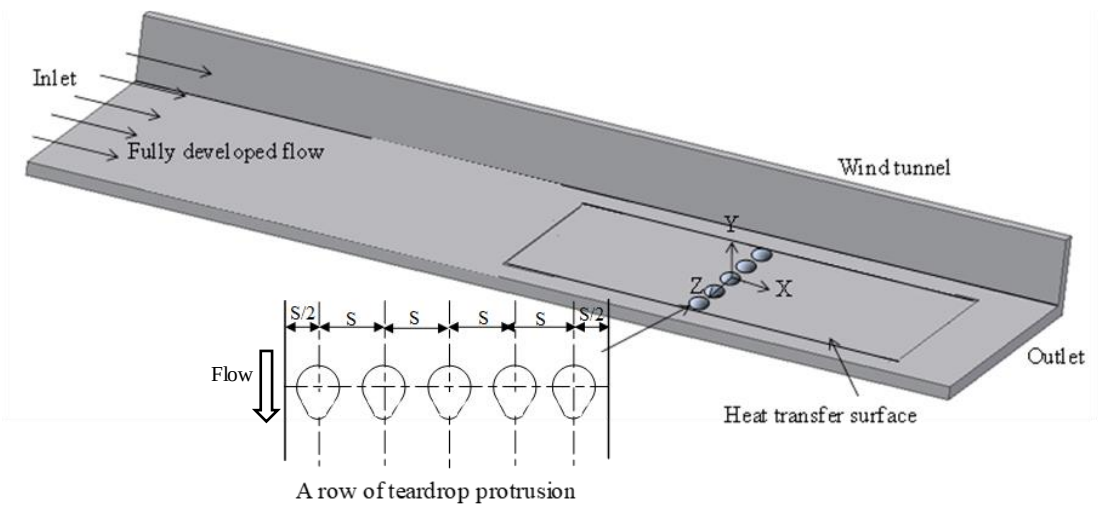

Figure 3. Experimental 3D model of wind tunnel with single teardrop protrusions row.

1.3. Measurement of heat transfer

The test section for heat transfer measurement is shown in figure 4. The heat transfer surface was made of a stainless-steel foil with thickness of 0.03mm. The foil was attached with Thermochromics liquid crystals sheet (TLC_S) on the side of the wall. The stainless-steel foil was stretched between a couple of copper bus bars. The heat transfer surface was heated by DC power source that can supply current through the copper bus bars. A digital camera was used to capture color on the TLC sheet. Images of color pattern on the TLC sheet were converted from a red, green, and blue (RGB) system to a hue, saturation, and intensity (HSI) system. The air was introduced through the inlet chamber, flow straightener, two layer of mesh plates, test section and chamber outlet by using blower.

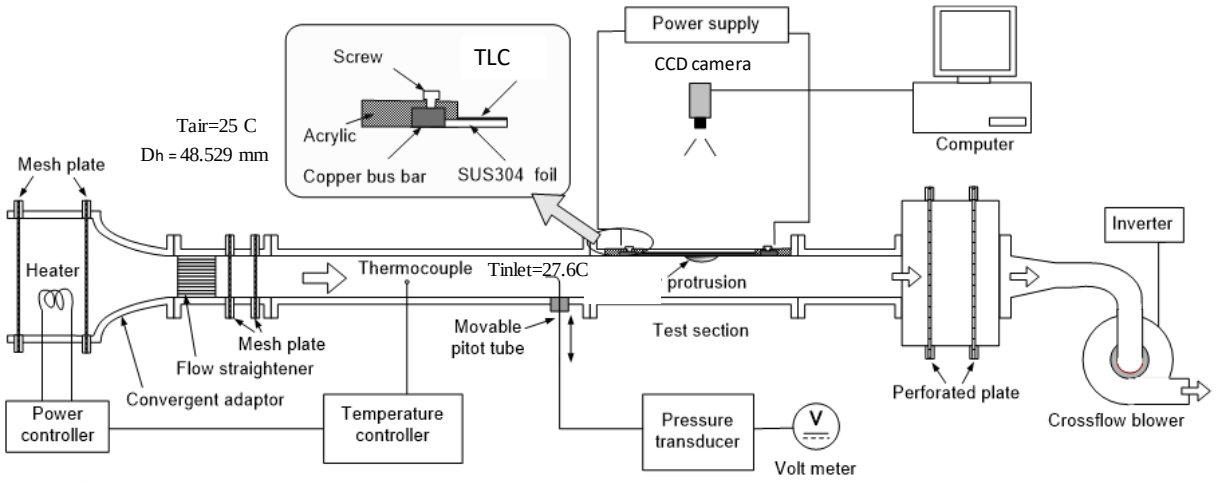

Figure 4. Schematic diagram of experimental set-up.

Electrical energy dissipated in the stainless-steel foil can be calculated from:

$$\dot{Q}_{input} = I^2 \cdot R \tag{1}$$

where, *I* is the supplied electrical current and *R* is the electrical resistance of stainless-steel foil.

The air temperature was controlled at 27.6°C and flow on the surface of stainless-steel sheet. The local heat transfer coefficient (*h*) can be calculated from this equation:

$$h = \frac{\dot{Q}_{input} - \dot{Q}_{losses}}{A(T_{LC} - T_a)} \tag{2}$$

where, $\dot{Q}_{input}$ is the rate of heat generation in the stainless plate, $\dot{Q}_{losses}$ is the rate of heat loss for convection and radiation, A is the area of heat transfer surface, T_{LC} is the temperature of the colour that appears on the TLC plate and T_a is air temperature.

The local Nusselt number can be calculated from

$$Nu = \frac{hD_H}{k} \tag{3}$$

where, D_H is hydraulic diameter and k is thermal conductivity of air.

3. Results and discussion

The contours and the values of Nusselt number on the surface of only three protrusions are described in figure 5. The solid part area of teardrop was not considered about Nusselt number. At the front edge of teardrop protrusion, low Nusselt number value was found because flow impingement became strong and this effect caused the small circulation flow region. In addition, the flow separation mainly occurred over the downstream half of teardrop protrusion surface, and the turbulent wake reattached immediately downstream of the protrusion. Low-pressure region formed in the rear section of protrusion and, the flow coming from two sides entered this region. Therefore, the distribution of high Nusselt number could be seen at the downstream of protrusions due to the flow separation and attachment flow immediately appeared along the downstream of protrusion [1, 5] and this effect can enhance heat transfer augmentation. Increasing or decreasing Nusselt number on the dimple and protrusion surface can occurr because of both attachment and circulation flow effects that was studied in literature [1, 4]. Furthermore, the results were found that the Nusselt number increased when the

protrusion-to-protrusion spacing decreased because of the flow tendency to the lateral side of longitudinal vortex pair between protrusion-to-protrusion spacing and turbulent flow.

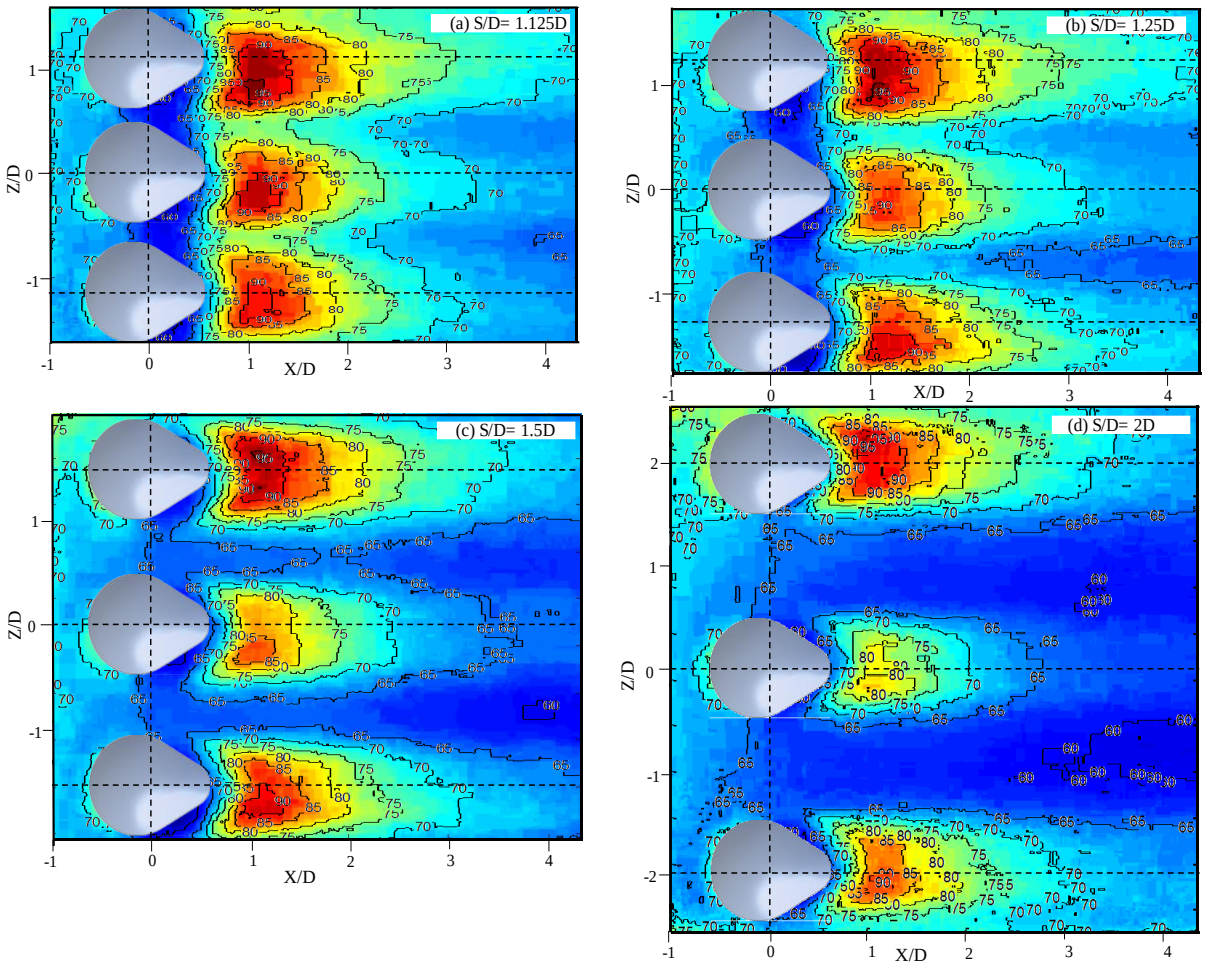

Figure 5. Contour of Nusselt number on teardrop protrusion surface.

The distribution of Nusselt number value along the protrusion centre Z/D=0 for all S/D cases was shown in figure 6. The area of the range ($-0.5 \leq X/D \leq 0.75$) was not considered because it is a protruded teardrop It was found that the maximum peak trend occurred at S/D=1.125 and this trend was higher than the other S/D cases.

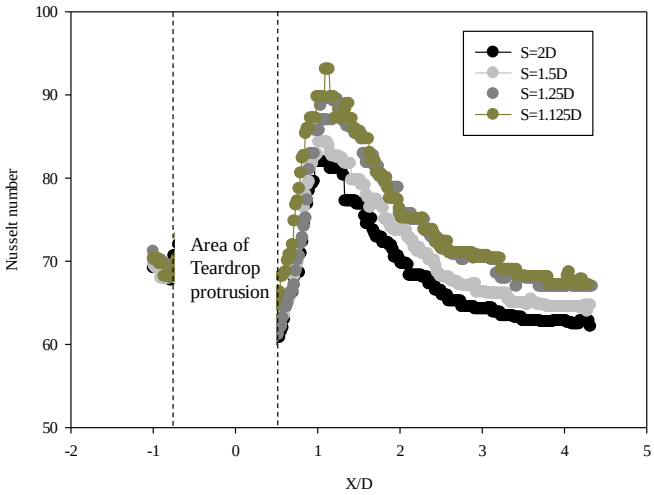

Figure 6. Nusselt number distributions in stream wise direction (*X/D*) (*Z/D*=0, Re_H=20,000)

Figures 7, 8 and 9 show the span wise Nusselt number distributions at the downstream portion of protrusion (*X/D*=1, 2 and 3) for all *S/D* cases. Three peak regions of maximum Nusselt number cases occurred behind the protruded teardrop smooth surface. When the distance downstream behind the protrusion became large, the value of Nusselt number became small because the reattachment flow was occurred at the position just behind the teardrop protrusion. It can be clearly seen that S/D=1.125 case was the highest Nusselt number distribution trend for every X/D cases among different spacing cases. In figure 7, the value of Nusselt number values for S=1.125D case was 75<Nu<100. However, the value of Nusselt number values for S=2D case was 60<Nu<95. In addition, the smallest spacing case (S=1.125D) can develop more turbulent wake and longitudinal flow compared to other cases.

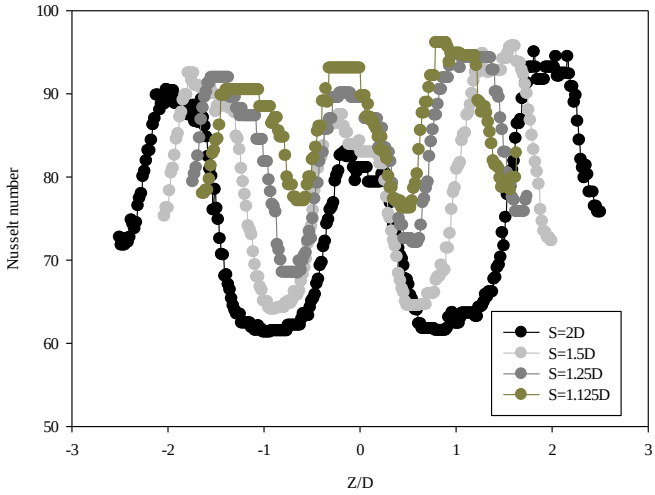

Figure 7. Nusselt number distributions in span wise direction (*Z/D*)) (*X/D*=1, Re_H=20,000).

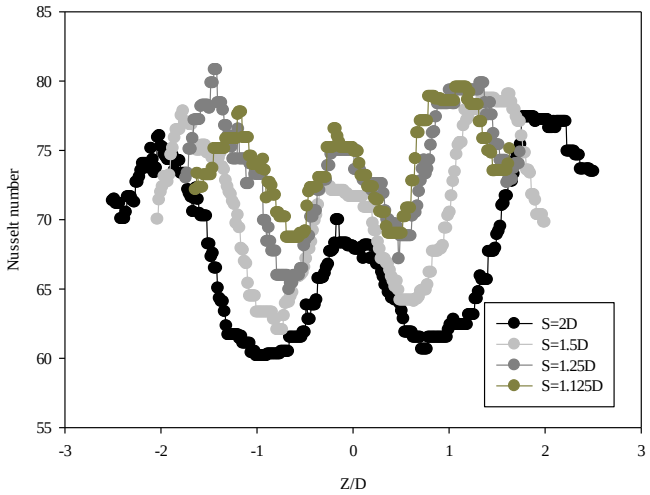

Figure 8. Nusselt number distributions in stream wise direction (*Z/D*) (*X/D*=2, Re_H=20,000).

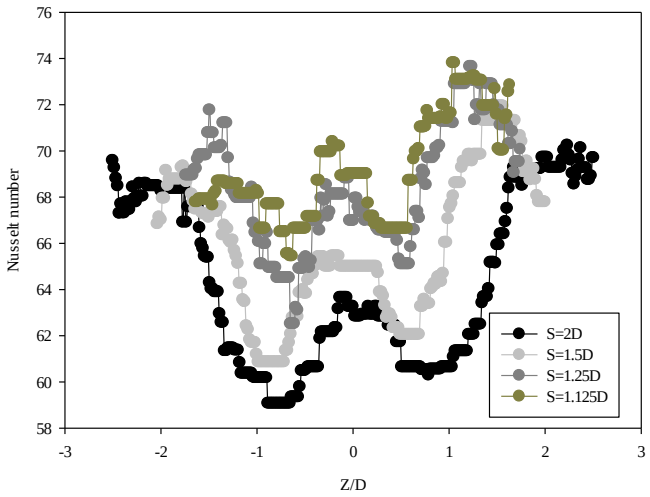

Figure 9. Nusselt number distributions in stream wise direction (*Z/D*) (*X/D*=3, Re_H=20,000).

The average stream wise Nusselt number distribution of respective spacing case is illustrated in figure 10. The trend of Nusselt number distribution for S=1.125D case was the highest Nusselt number. The position of 0.5<X/D<2 was the highest Nusselt number region because the reattachment flow happened in this area. Moreover, figure 11 shows the average Nusselt number over protrusion surface of evaluated heat transfer area. The value of average Nusselt number was 71.287 for S=1.125D case while the other cases were 70.467, 68.617 and 66.837. The result can be shown that the trend of average value become low when *S/D* become large. The highest average Nusselt number case was the narrowest spacing case (*S/D*=1.125*D*).

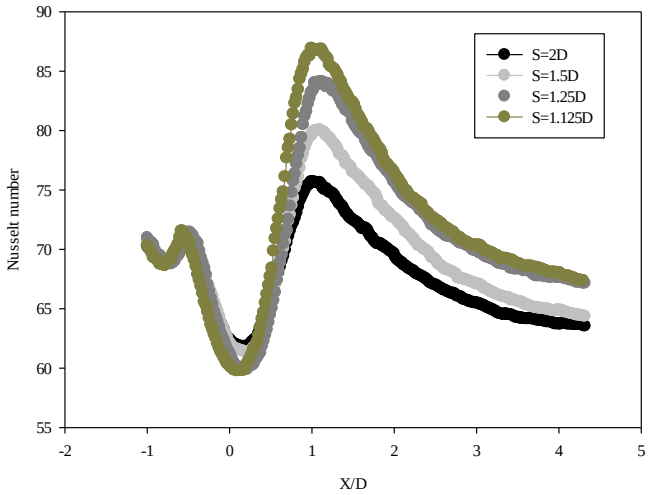

Figure 10. Nusselt number distributions in streamwise direction (X/D) (-2.4<Z/D<2.4 for S=2D, -2<Z/D<2 for S=1.5D, -1.7<Z/D<1.7 for S=1.25D, -1.6<Z/D<1.6 for S=1.125D, Re_H=20,000).

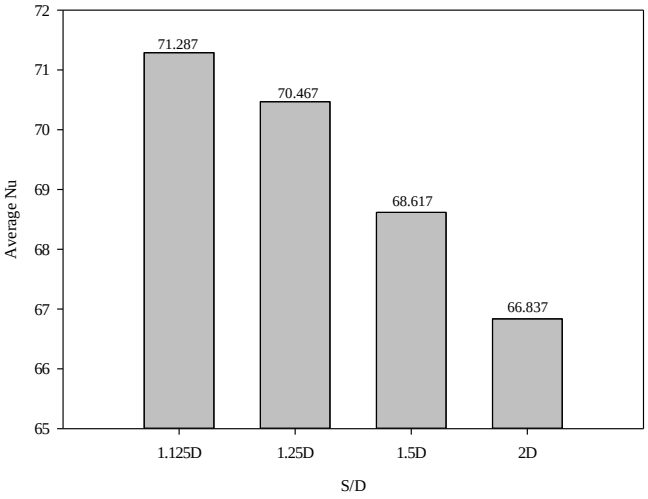

Figure 11. Average Nusselt number of teardrop protruded test section surface (Re_H=20,000).

4. Conclusions

In this work, the investigation of heat transfer characteristics over the teardrop protrusion surface of evaluated heat transfer area in wind tunnel was studied. The spacing was varied with different spacing at S/D=1.125, 1.25, 1.5 and 2. The summery of this work are as follows:

1. The value of average Nusselt number was increased when protrusion-to-protrusion spacing was decreased. The highest Nusselt number average value can be found in S/D=1.125 case.
2. The heat transfer was low at just in front of the protrusion due to circulation flow that appeared in this region. The region downstream of protrusion, the heat transfer was high because of reattachment flow.
3. The high Nusselt number can be observed at the position for the downstream of protrusion (X/D=1) because of reattachment flow after that Nusselt number values became low along the downstream of smooth surface.

Acknowledgement
The research grant was supported by the Research and Development Office (RDO), Prince of Songkla University, grant No. ENG590725S.

References
[1] Acharya S and Zhou F 2012 *J. Turbomach.* **134** pp 0610281– 06102813
[2] Xie Y, Qu H and Zhang D 2015 *Int. J. Heat Mass Transf.* **84** pp 486–496
[3] Chang S W, Chiang F, Yang T L and Huang C C 2008 *Exp. Therm. Fluid Sci* **33** pp 23–40
[4] Li P, Zhang D and Xie Y 2014 *Int. J. Heat Mass Transf.* **73** pp 456–467
[5] Rao Y, Li B and Feng Y 2015 *Exp. Therm. Fluid Sci* **61** pp 201–209
[6] Mohammad A E and Danesh K T 2008 *J. Turbomach.***130** pp 0410161–0410169
[7] Wae-Hayee M, Tekasakul P, Eiamsa-ard S and Nuntadusit C 2015 *Experiment of Heat Transfer* **28** pp 511–530